

Recombination processes in *a*-Si:H: Spin-dependent photoconductivity

H. Dersch, L. Schweitzer,* and J. Stuke

Department of Physics, University of Marburg, D-3550 Marburg, Federal Republic of Germany

(Received 21 December 1982; revised manuscript received 28 February 1983)

We report on photoconductivity measurements and on the resonant photoconductivity change induced by ESR in undoped *a*-Si:H in the temperature range 100–300 K. We investigate samples with various defect densities (5×10^{15} – 10^{18} cm⁻³) which are achieved by electron bombardment and subsequent annealing. Samples with a high-defect density ($N_s > 10^{17}$ cm⁻³) exhibit a resonant quenching effect which is attributed to spin-dependent tunneling of localized band-tail electrons to singly occupied defect states (dangling bonds). In low-defect material an additional quenching resonance is observed which is identified with spin-dependent diffusion (thermalization) of localized band-tail holes to doubly occupied dangling bonds. The results confirm our recombination model in which trapped electrons and holes recombine via defect states by tunneling and diffusion rather than by capture of free carriers.

I. INTRODUCTION

Recombination processes in *a*-Si:H have been studied extensively by various experimental techniques, in particular by luminescence and photoconductivity measurements. Recently, magnetic-field-dependent photoconductivity (MDP),¹ magnetic-field-dependent luminescence (MDL),² spin-dependent photoconductivity (SDPC),^{3,4} and optically detected magnetic resonance^{5–8} (ODMR) have elucidated several processes involved in recombination. In MDP and MDL the information is solely contained in the magnitude of the photoconductivity or luminescence change due to the application of an external static magnetic field, and thus not easy to extract, whereas ODMR and SDPC experiments permit far more insight into the dynamics of the system and in particular exhibit the *g* values of the spin centers involved in the recombination transitions. SDPC and ODMR investigations on *a*-Si:H are carried out by recording the change in photocurrent or luminescence intensity as the material is brought into microwave resonance due to application of microwave power and a magnetic field.

Although a large amount of information has been accumulated, a generally accepted model capable of describing all the effects observed has not yet been presented. One problem is inherent in the complexity of the considered problem itself, since several possible competing recombination paths have to be treated simultaneously. The main difficulty, however, seems to be the identification and interpretation of the observed resonance spectra which are very sensitive to experimental conditions and in fact strongly influenced by various parameters, e.g., by microwave power, modulation frequency, chopping frequency, phase set, excitation intensity, etc. This basic problem is reflected in the disagreement of results reported by various groups for ODMR on *a*-Si:H.^{5–9} While the ODMR results were obtained by measuring the luminescence change and therefore restricted to low temperatures, we report here on the resonant photocurrent change (SDPC) at higher temperatures. Though our experiments are similar partly to those performed earlier,^{3,4,10} the results and conclusions differ appreciably.

At first a few general remarks should be made. As

mentioned above, the great advantage of ODMR and SDPC experiments over the simpler MDL and MDP investigations is the fact that in principle one directly observes the electronic states taking part in the recombination processes. This requires, however, the states to be paramagnetic and in addition the exchange interaction to be weak since otherwise the characteristic *g* values, which allow us to identify the centers involved, are blurred. Furthermore, the dominant recombination transitions have to be spin dependent, which means that the spin-selection rules crucially enter the transition probability. For thermalized spins the recombination process has a normal spin dependence, i.e., the spin-spin coherence time τ_c is short compared with the transition time (hopping or recombination time). Then only the well-known polarization effect is to be expected at low temperatures.^{11,12} In the case of unthermalized spins, when the spin coherence time is long compared with the transition time, the recombination or hopping process is delayed if the spins are parallel. A static magnetic field or an additional microwave field destroy the correlation between the spins and as a result the recombination or hopping rate increases. This anomalously spin-dependent process was suggested for the first time in connection with the magnetoresistance¹³ and magnetophotoconductivity problems¹ and applies also to the ODMR and SDPC experiments.^{11,12}

The main difference between detecting either the change in luminescence intensity or in photocurrent is that in the case of luminescence, one has to consider both radiative and nonradiative processes, while there is no distinction to be made in the case of photocurrent. This is so because enhancing the recombination by microwave resonance decreases the photocurrent irrespective of whether the process is radiative or nonradiative. The different temperature ranges for observing luminescence and photoconductivity have also to be taken into account. In the following we propose a model for recombination in amorphous hydrogenated silicon which is based on the photoconductivity investigations presented below. One of our results is the inclusion of a new recombination step, namely the diffusion of localized band-tail holes to doubly occupied dangling bonds.

II. EXPERIMENT

A. Samples

The samples of *a*-Si:H have been prepared by plasma decomposition from a 20:1 He-SiH₄ mixture. For conductivity measurements thin films, typically 1 μm thick, were deposited onto quartz substrates. The conductivity was measured between two chromium electrodes, 0.3 mm apart. For ESR measurements layers with a thickness of about 10 μm were deposited onto thin molybdenum foils and by bending peeled off from the substrate. The measured ESR line is the usual dangling-bond resonance ($g = 2.0055$, linewidth $\Delta H_{pp} = 7$ G) and the spin density is $5 \times 10^{15}/\text{cm}^3$. To study the influence of different defect densities on the photoconductivity additional dangling bonds were introduced by electron bombardment. Electron irradiation was carried out at the Kernforschungsanlage Jülich (fluence 6×10^{13} electrons $\text{cm}^{-2} \text{s}^{-1}$, temperature 4 K, energy 3 MeV, electron dose 2×10^{19} electrons cm^{-2}). Since the penetration depth of these electrons is much larger than the thickness of the samples,¹⁴ defects are created uniformly throughout the material. The shape of the ESR absorption and the g value do not vary upon irradiation but the spin density increases up to $N_s = 10^{18}/\text{cm}^3$. Annealing at 220 °C reduces the spin density to its original value. Therefore, the concentration could be easily varied in the range $5 \times 10^{15}/\text{cm}^3$ to $10^{18}/\text{cm}^3$ by electron bombardment and stepwise annealing.

B. Photoconductivity

Photoconductivity measurements were carried out by illumination with a tungsten-iodine lamp at an incident power of 50 mW/cm². In Fig. 1 the photoconductivity of an electron-bombarded sample is plotted as a function of temperature. The lowest curve is obtained after electron irradiation and annealing at room temperature

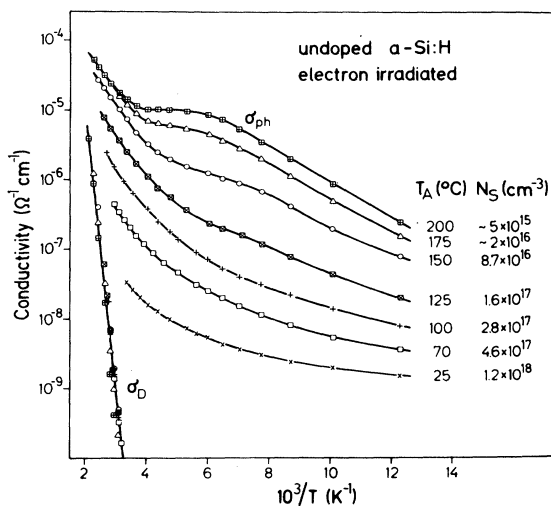


FIG. 1. Photoconductivity σ_{ph} and dark conductivity σ_d of electron-bombarded *a*-Si:H after different annealing temperatures.

($T_A = 25$ °C). After stepwise annealing at higher temperatures (annealing time 30 min), the photoconductivity increases by about 3 orders of magnitude and reaches at $T_A = 200$ °C the original value obtained before irradiation. The temperature dependence of the photoconductivity also changes by annealing. In high-defect material ($T_A < 125$ °C, $N_s > 2 \times 10^{17}/\text{cm}^3$), the photoconductivity increases monotonically with temperature. Low-defect material ($T_A > 150$ °C, $N_s < 10^{17}/\text{cm}^3$) has a shoulder at about $T = 200$ K, which increases as the defect density is reduced. It is relevant that those samples exhibit infrared quenching of the photoconductivity below this temperature.¹⁵

The dependence of σ_{ph} on light intensity I was investigated in the range $0.2 \text{ mW/cm}^2 < I < 80 \text{ mW/cm}^2$. Over the whole temperature range and at all defect concentrations monomolecular recombination kinetics have been observed. The exponent ν in the relation $\sigma_{ph} \propto I^\nu$ lies in the range 1 ± 0.05 .

The dark conductivity σ_d is also plotted in Fig. 1. In contrast to σ_{ph} the dark conductivity is only a little affected by electron bombardment and subsequent annealing. We always obtain straight lines with an activation energy of 0.85 ± 0.03 eV; only the highest-defect sample shows some deviation from an activated behavior, which may be due to hopping contributions to σ_d . We conclude, therefore, that independent of the defect concentration the dark Fermi level E_F always remains near midgap, i.e., the defect levels introduced by irradiation also lie in this energy range. Since σ_{ph} strongly depends on the position of E_F it is important to decide whether the reduction of σ_{ph} by irradiation is due to the higher-defect density or to a shift of E_F towards the middle of the gap. Since we started with samples having E_F in midgap position before electron bombardment, we can exclude doping effects. This is not the case in samples with activation energies below 0.85 eV, where E_F shifts considerably by creating defects.

C. Spin-dependent photoconductivity (SDPC)

The spin-dependent measurements were carried out in a usual ESR spectrometer (Varian E 12). The sample was mounted in a microwave cavity and illuminated through slots in the cavity wall. While employing the full microwave power of the ESR bridge (200 mW) the photo-current I_{ph} was monitored as a function of the static magnetic field H_0 . A resonant decrease of I_{ph} has been observed at a magnetic field H_0 which corresponds to a g value lying close to the well-known ESR defect states. To improve sensitivity, H_0 was modulated and I_{ph} detected with lock-in technique. As in ESR spectroscopy one obtains the derivative of the signal with respect to H_0 thus providing a convenient way to compare with the ESR-absorption line shapes. The modulation frequency normally was 200 Hz. The temperature could be varied in the range 100–350 K by cooling with dry nitrogen; the accuracy of T is about ± 3 K.

It is useful to compare the recorded SDPC spectra with ESR line shapes of doped *a*-Si:H.¹⁷ In Fig. 2 typical ESR spectra are illustrated which have been attributed to different gap states. Three resonances have been identified and the energetic range of the corresponding gap states is shown in the lower part of Fig. 2: midgap states, which

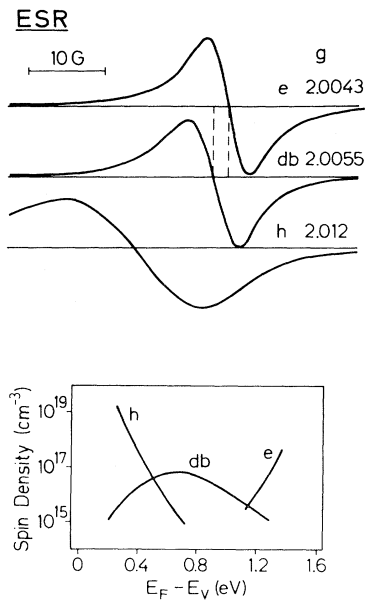


FIG. 2. Derivative of the ESR absorption line shapes of conduction-band-tail electrons (*e*), valence-band-tail holes (*h*), and defect states [dangling bonds (*db*)]. The energetic distribution of the corresponding gap states is shown below (spin density vs position of the Fermi level E_F).

carry a spin when neutral [dangling bonds (*db*), $g=2.0055$, linewidth $\Delta H_{pp}=7$ G]; conduction-band-tail states, carrying a spin after electron capture [trapped electron (*e*), $g=2.0043$, $\Delta H_{pp}=6$ G]; valence-band-tail states, carrying a spin after hole capture [trapped hole (*h*), $g=2.009-2.013$, $\Delta H_{pp}=12.5-20$ G].

As in the case of the photoconductivity (Fig. 1) the SDPC results show a clear distinction between samples with high- and low-spin densities. In samples with high-defect densities ($N_s > 2 \times 10^{17}/\text{cm}^3$) a single unstructured line is found; samples with lower-defect densities, however, show more complicated spectra. In the upper part of Fig. 3 the SDPC line shape is shown which is obtained for samples with $N_s > 2 \times 10^{17}/\text{cm}^3$. The linewidth ΔH_{pp} is 11 G and the g value 2.0050. Line shape and g value are independent of temperature in the range investigated. The dashed vertical lines in Fig. 3 indicate the ESR g values of the *e* and *db* line. The g value of the SDPC line lies close to the middle between those of the two single ESR lines. We therefore conclude that the SDPC line shape is a superposition of the *e* and *db* resonances. This is demonstrated in the lower part of Fig. 3, where the superposition of these two lines is shown which again is an unstructured line having the correct g value. However, the linewidth is smaller (7 G) which is probably due to the lower microwave power P applied in the ESR experiments. Thus the physical interpretation of the SDPC line shape is obvious: The process observed in high-defect material is tunneling of trapped band-tail electrons to neutral dangling bonds.

The intensity of the line (maximum value of $\Delta\sigma_{ph}/\sigma_{ph}$ induced by the microwave) decreases slightly with increasing temperature (Fig. 4). It is important that the relative

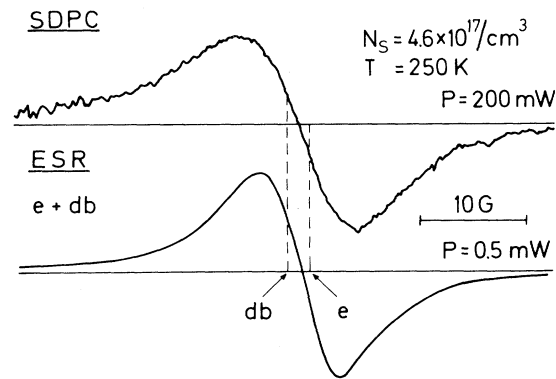


FIG. 3. SDPC spectrum of high-defect *a*-Si:H and computed superposition of *e* and *db* ESR spectra.

change $\Delta\sigma_{ph}/\sigma_{ph}$ has the same magnitude and temperature dependence for all four samples shown in Fig. 4 whereas the absolute values σ_{ph} (and $\Delta\sigma_{ph}$) differ clearly (see Fig. 1). This provides strong evidence that the observed tunnel process is the dominant recombination mechanism. If the spin-dependent process were only a minor recombination channel it would be hard to understand why $\Delta\sigma_{ph}$ increases in the same way as σ_{ph} itself when the spin density is reduced. The relative change $\Delta\sigma_{ph}/\sigma_{ph}$ is independent of light intensity in the range $1 \text{ mW}/\text{cm}^2 < I < 40 \text{ mW}/\text{cm}^2$.

Street obtained similar results from recent ODMR measurements performed at low temperatures.⁹ Our data show that the tunnel processes of trapped band-tail electrons to dangling bonds dominate the recombination lifetime in high-defect *a*-Si:H also in the high-temperature range (100–300 K).

By reducing the defect density below values of $10^{17}/\text{cm}^3$ the signal intensity decreases and the line shape changes, indicating that the recombination mechanism is different in low-defect samples. The presentation of the low-defect material will be restricted to the as-deposited sample with the lowest spin density ($N_s = 5 \times 10^{15}/\text{cm}^3$). The samples with spin densities between $5 \times 10^{15}/\text{cm}^3$ and $10^{17}/\text{cm}^3$ show a continuous transition from the behavior described

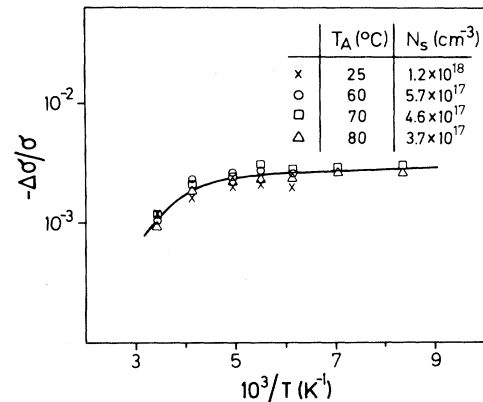


FIG. 4. Temperature dependence of $\Delta\sigma/\sigma$ in high-defect *a*-Si:H.

above to that described now. SDPC spectra of low-defect material change remarkably with increasing temperature as can be seen from Fig. 5. The dashed lines correspond to the *g* values of the ESR resonances. The spectra are obviously superpositions of all three ESR lines; at $T = 125$ K one can clearly see the hole line *h* together with the *e* and/or *db* line. To higher temperatures the lines start to merge and at room temperature a single line with $g = 2.0057$ is observed.

It was pointed out by Schiff⁴ that high-frequency modulation ($\nu > 1$ kHz) of the magnetic field yields a quadrature spectrum with different *g* value and line shape than the in-phase spectrum. We used these relaxation effects to separate the processes which lead to the complicated line shape. In Fig. 6 SDPC spectra at a higher modulation frequency ($\nu = 1$ kHz) are plotted for three different phase settings of the signal channel of the lock-in amplifier. Comparison of the in-phase spectrum (a) with the spectrum of Fig. 5 ($T = 150$ K) shows that the intensity of the broad component is reduced at higher modulation frequency. Figure 6(b) shows the quadrature spectrum, which is a broad asymmetric line with $g = 2.01$. The same *g* value is obtained by subtracting spectrum 6(a) from the corresponding low-frequency modulation spectrum (Fig. 5) indicating that only the broad component is affected by high-frequency modulation. The broad signal vanishes at the phase set of -105° [Fig. 6(c)], the remaining signal being a narrow line similar to that found in high-defect samples ($g = 2.0050$). It should be mentioned that for high-defect material no change of line shape upon phase setting could be observed up to the highest available modulation frequencies (10 kHz). Hence the SDPC spectrum of Fig. 6(a) can be separated into two components with different dynamics: a slow process ($g = 2.01$), which is shifted in phase ($\sim 15^\circ$) at $\nu = 1$ kHz thus leading to a quadrature signal, and a fast process not observed in the quadrature spectrum. From the decrease in signal intensi-

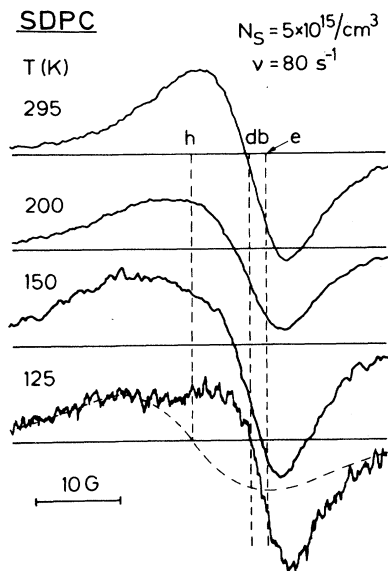


FIG. 5. SDPC spectra of low-defect *a*-Si:H at various temperatures. Magnetic field modulation frequency $\nu = 80$ Hz.

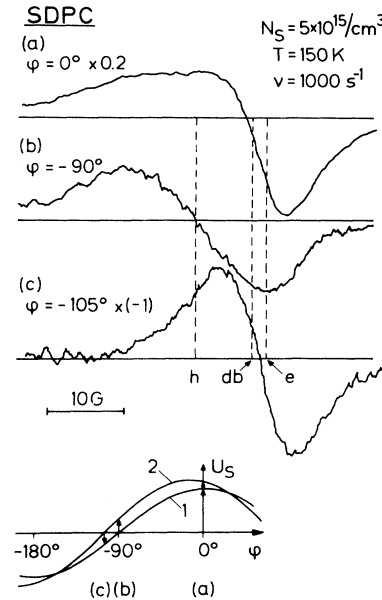


FIG. 6. SDPC spectra of low-defect density *a*-Si:H at $T = 150$ K for different phase settings ϕ of the lock-in amplifier. Magnetic field modulation frequency $\nu = 1000$ Hz. The lower part shows the output voltage of the lock-in amplifier as a function of phase setting ϕ ; (a), (b), and (c) denote the corresponding spectra shown above.

ty and the phase shift of the broad resonance we roughly estimate the time constant of the slow process to be 5×10^{-5} s. The narrow line does not change in the available frequency range, which gives an upper limit of 2×10^{-6} s for the time constant of the fast process.

In the lower part of Fig. 6 it is demonstrated schematically how the recorded spectra depend on the phase setting ϕ . Curve 1 shows the dependence of the output voltage of the lock-in amplifier, if the signal can follow the modulation simultaneously. This is obviously the case for the *e*-*db* resonance. Curve 2 shows the output signal for a process, which is shifted in phase relative to the reference signal, as it is the case for the broad resonance at high-modulation frequencies. The whole spectrum is a superposition of the two signals, but the signals can be detected separately with the settings $\phi = -90^\circ$ [Fig. 6(b)] and $\phi = -105^\circ$ [Fig. 6(c)], respectively.

A separation of the SDPC spectra similar to Fig. 6 has been carried out for different temperatures. Even at room temperature a quadrature signal was observed ($\nu = 1$ kHz). However, the difference ϕ between the quadrature angle and the phase where the narrow line is observed isolated decreases from 15° at $T = 150$ K to about 8° at 300 K, indicating that the time constant of the slow process decreases to 3×10^{-5} s at high temperatures. In the lower part of Fig. 7, linewidth and *g* value of the two components are demonstrated as they are observed in the quadrature spectrum and at a phase set of $(-90^\circ - \phi)$, respectively. The circles correspond to the in-phase component (*e*-*db* line) and the triangles to the phase-shifted broad line. The *e*-*db* line does not change its line shape and *g* value over the whole temperature range

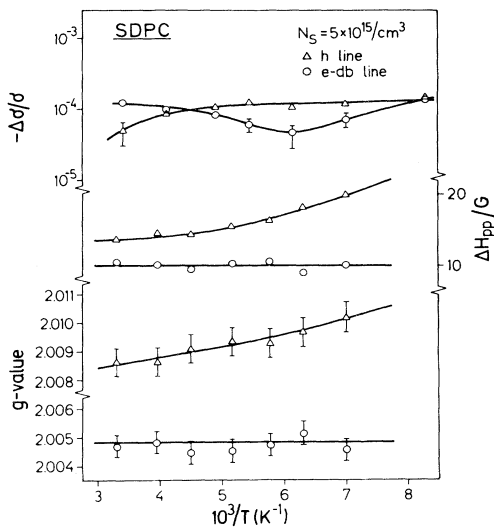


FIG. 7. Intensity, g value, and linewidth of the h line (Δ) and the e -db line (\circ) in low-defect a -Si:H as a function of temperature.

($g=2.0050$, $\Delta H_{pp}=10$ G) similar to the spectra of the high-defect material. The linewidth of the broad resonance, on the other hand, decreases from 20 G at 125 K to 13.5 G at 295 K. Correspondingly, the g value decreases from 2.01 to 2.0085.

In the upper part of Fig. 7 the intensities $\Delta\sigma_{ph}/\sigma_{ph}$ of the two lines are shown. These intensities are obtained by fitting the in-phase spectra at low-modulation frequencies (Fig. 5) numerically with the two components mentioned above. $\Delta\sigma/\sigma$ is about a factor of 20 smaller than in high-defect samples. For the broad line $\Delta\sigma/\sigma$ is constant up to 250 K and then decreases monotonically. The e -db line first decreases with increasing temperature but above 250 K it increases. At 350 K only the e -db line could be detected; i.e., at high temperatures the sample behaves like high-defect-density material. However, $\Delta\sigma_{ph}/\sigma_{ph}$ is not independent of light intensity at low temperatures but decreases with increasing illumination, the decay of the e -db line being stronger than that of the h line.

The question arises whether the deconvolution of the signal is unique. Mathematically this is not the case, because two spectra obtained for arbitrarily chosen phase angles may be used to construct the line. Physically there are some distinguished phase sets, especially the quadrature angle, where the fast in-phase components disappear. Once having the quadrature spectrum, the fast signal can be detected by finding the angle, where the broad resonance vanishes. Again this method is not unique in a mathematical sense, and any other but the above angle could be chosen to get a second signal. However, in any case this would imply that the broad resonance takes part in the fast in-phase process, too. Then it would be hard to understand why the broad resonance decreases at high modulation frequencies just as at high temperatures whereas the narrow signal remains almost constant. Since the relaxation phenomena observed in the spectra are easily explained by assuming the two above-mentioned processes we believe our deconvolution to be correct.

The g value and linewidth of the broad component indicate that trapped holes are involved in this process. Since both ESR resonances of the centers which take part in the spin-dependent transition should appear in the spectrum, the second center is either a trapped hole too, or a trapped electron or dangling bond not resolved in the spectrum. This could be the case if the spins of the two centers form an exchange-coupled pair. Then the g value and linewidth of the resulting resonance would lie in between those of the two single resonances. However, exchange-coupled pairs of band-tail holes and dangling bonds (or band-tail electrons) have never been observed in ESR spectra of a -Si:H. In the ESR spectra of boron-doped a -Si:H, for instance, high densities of singly occupied dangling bonds and valence-band-tail states ($N_s > 10^{17}/\text{cm}^3$) can be resolved separately, indicating that the exchange interaction is rather weak. In light-induced ESR (LESR), the same is true for the e and h resonances. In SDPC, on the other hand, one detects only those centers which are close enough to make transitions. Therefore, in certain cases exchange-coupled spins may dominate the recombination whereas decoupled spins are observed in ESR. For example, Street⁹ assigned a broad enhancing ODMR line, with $g=2.009$ and $\Delta H_{pp}=17$ G observed below 80 K, to exchange-coupled pairs of trapped electrons and holes which recombine radiatively. Since luminescence is strongly quenched above 120 K this transition will surely be negligible in the case of SDPC. Moreover, Movaghar *et al.*¹¹ pointed out that exchange interaction within the pairs destroys the influence of the microwave on the recombination since in this case the singlet and triplet levels are split off and the microwave only induces transitions between the three triplet levels which do not influence the recombination rate significantly. These authors conclude that in the case of strong exchange interaction the SDPC signal will disappear. Finally, the line shape of the broad resonance itself (especially at low temperatures) which completely resembles the ESR hole line is hard to understand by mixing the h line with one of the two narrow ESR signals.

Therefore, we prefer our first interpretation given above and suggest that tunneling transitions between trapped localized holes act to reduce the photoconductivity. These processes will occur during thermalization and diffusion, i.e., the microwave radiation increases the mobility of trapped holes. Since the valence-band-tail states can be differently charged (neutral, singly, and doubly positive) only a part of the possible transitions is spin dependent, namely those between two singly occupied states. The total spin dependence of the hole-diffusion process thus depends on the relative occupancy of positively charged and neutral tail states in the energetic range where diffusion takes place. From recent LESR measurements we estimate that about $2 \times 10^{17}/\text{cm}^3$ trapped holes are present in our lowest-defect samples at $T=120$ K and comparable excitation intensities. We achieve similar concentrations of singly occupied tail states in the dark by boron doping with $[\text{B}_2\text{H}_6/\text{SiH}_4]=2 \times 10^{-3}$ which shifts the Fermi level to about 0.45 eV above the valence-band edge E_v . These samples exhibit a large anomalous change of the dark conductivity in the presence of a magnetic field¹⁸ which has been explained by spin-dependent hopping at the Fermi level, i.e., by spin-dependent transitions between valence-

band-tail holes. Moreover, in recent experiments we have identified spin-dependent hole diffusion in boron-doped *a*-Si:H ($[B_2H_6/SiH_4]=7.5 \times 10^{-3}$) by measuring the resonant change of dark conductivity induced by ESR. At low temperatures ($T < 180$ K) a broad enhancing line with $g=2.01$ (linewidth 18 G) is found which again resembles the corresponding ESR hole line as well as the broad quenching line found in SDPC of undoped *a*-Si:H with low-defect density. This provides additional support to our assumption that a great part of the hole-diffusion steps are spin dependent and thus can be influenced by microwave radiation.

The g value and linewidth of the SDPC h line decrease with increasing temperature (Fig. 7). A similar change in the ESR h resonance has been observed upon increasing boron doping^{17,19} which has been explained by distribution of g values of the corresponding valence-band-tail states. States which are closer to the valence-band edge exhibit smaller g values than those deeper in the gap. The dark Fermi level of the boron-doped samples as derived from dark conductivity gives a rough estimate of the energy which corresponds to a given g value. From the ESR results we conclude that the energy of the hole states, which take part in the spin-dependent transitions observed in SDPC, is about $E_v + 0.45$ eV at $T=125$ K decreasing to $E_v + 0.3$ eV at $T=300$ K. This energy corresponds to the range where the major part of the hole diffusion takes place. A model for the recombination which accounts for the various processes observed in the SDPC spectra will be given in the next section.

III. THE MODEL AND CONCLUSIONS

The recombination model is essentially based on our previously published considerations concerning the density of states in the gap of *a*-Si:H. Taking into account the important correlation effects as deduced from ESR experiments,^{17,19} we proposed that apart from the localized conduction- and valence-band-tail states only one defect state is present in order to account for the features observed in the field-effect density of states.²⁰ This defect is the dangling bond, which can be positively charged when unoccupied (D^+), neutral (singly occupied) (D^0), and negatively charged (doubly occupied) (D^-). It has a correlation energy $U \sim 0.4$ eV.^{17,21}

The photoconductivity in undoped *a*-Si:H is governed by electrons above the mobility edge E_c . Contributions to the photocurrent from holes will be very small since the hole traps are by about a factor of 2 deeper than the electron traps. We believe that this difference is due to the larger correlation energy U of the corresponding valence-band-tail states. Our model for the various recombination steps is described in Fig. 8. After creation, electrons (n_e) and holes (n_h) are trapped in localized band-tail states (e, h) from where they are either reemitted into the conducting states above the mobility edges or eventually recombine via defect states. It will be shown below that direct recombination of free carriers into defect states can be neglected for our material. Then the relevant recombination steps are as follows: Trapped electrons tunnel to neutral dangling bonds D^0 with a rate $r_e D^0$, which is a spin-dependent transition and leads to the e -db resonance observed in SDPC spectra of both high- and low-defect-

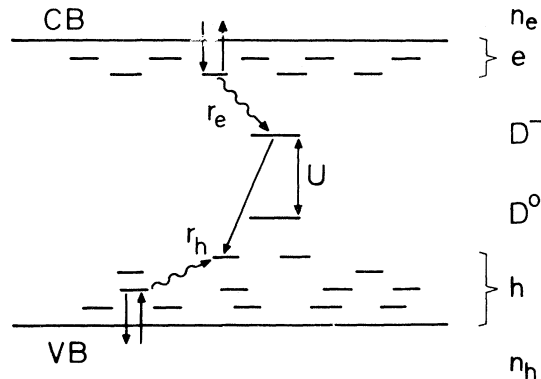


FIG. 8. Recombination scheme for *a*-Si:H. Wavy arrows indicate spin-dependent transitions.

density material. The next step is a transition from the doubly occupied and negatively charged defect state D^- to the trapped hole with rate $r_h D^-$. This rate may be enhanced by diffusion of the trapped holes via singly occupied tail states ($U \sim 0.2$ eV) towards the D^- defects, which is a spin-dependent process leading to the single h line in SDPC spectra. One might argue that the latter process is unlikely because the density of singly occupied tail states is small compared to the neutral doubly occupied states. Also, the Coulomb repulsion should make the transition to such a state more difficult. The first objection is weakened by the following considerations. If there were only one singly occupied site with antiparallel spin on each percolation path, the hole diffusion would be effectively blocked since the hopping times are shorter than the spin-lattice relaxation times. Hence a slower alternative route has to be chosen. This delay can be avoided by resonant microwave-induced spin flips. The magnitude of this effect depends on several physical quantities and is not easily estimated. However, measurements of the change in dark conductivity of boron-doped *a*-Si:H induced by magnetic fields as well as by ESR exhibit an appreciable effect as mentioned above. These experiments clearly demonstrate the existence and importance of spin-dependent hole diffusion. The second objection (Coulomb repulsion) is repudiated by the fact that after creation a diffusing hole has an enormous amount of excess energy. Thus, while thermalizing downward in energy, the Coulomb repulsion is no effective restriction unless the hole has completely thermalized. In this case a hole at site i hops only to such singly occupied sites j with energy difference $\epsilon_j - \epsilon_i + U < kT$, which is easily accomplished due to the broad distribution of the site energies.

The essential steps of the recombination sequence are described by the following rate equations:

$$\dot{n}_e = g - tn_e + de, \quad (1)$$

$$\dot{e} = tn_e - de - r_e e D^0, \quad (2)$$

$$\dot{D}^0 = r_h h D^- - r_e e D^0, \quad (3)$$

where we have assumed that $D^+ < D^0$. The generation rate, electron trapping, and reemission rates are denoted by g , t , and d , respectively. The density of defects is $D = D^0 + D^- + D^+$ and the steady-state solution is given

by

$$n_e = \frac{g}{t} \left[\frac{d(r_e e + r_h h)}{r_e r_h h D} + 1 \right]. \quad (4)$$

By applying a resonant microwave field we alter the transition probabilities: r_e is enhanced to $r_e + \Delta r_e$ by the e -db resonance and r_h increases to $r_h + \Delta r_h$ by improving the diffusion of holes (h resonance). The relative change in photoconductivity by ESR $\Delta\sigma_{\text{ph}}/\sigma_{\text{ph}}$ can now be expressed by the relative change of the recombination probabilities $\Delta r/r$ using Eq. (4) with the assumptions $d > r_e D^0$ (high temperature) and $n_e, n_h > D^-$ (undoped a -Si:H); i.e., the Fermi energy lies in between the D^0 and D^- levels,

$$\frac{\Delta\sigma_{\text{ph}}}{\sigma_{\text{ph}}} \simeq - \frac{1}{r_h + r_e} \left[\frac{\Delta r_e}{r_e} r_h + \frac{\Delta r_h}{r_h} r_e \right]. \quad (5)$$

We obtain two contributions to $\Delta\sigma_{\text{ph}}/\sigma_{\text{ph}}$. Depending on the weighting factors r_e and r_h the SDPC spectrum reflects the slowest transition. In the case of high-defect a -Si:H this is the tunneling of band-tail electrons to neutral dangling bonds (r_e) whereas in low-defect material the diffusion of holes becomes comparable at low temperatures (r_h) (see Figs. 4 and 7). This behavior can easily be understood by the following considerations: In low-defect-density material ($N_s < 10^{17}/\text{cm}^3$) the mean separation l of the dangling-bond sites is large, $l < 200$ Å, so that diffusion to the defect centers is more efficient than a single tunneling transition. Thus both the spin-dependent final step of the electron as well as the spin-dependent diffusion process of the hole show up in the resonant photoconductivity change. For high-defect-density material, on the other hand, a single tunneling transition to the nearby defect center is sufficient so that only the e -db transition is observed since direct tunneling of a hole to the doubly occupied dangling bond is not spin dependent. This is exact-

ly what is observed experimentally.

In the temperature range investigated, $d > r_e D^0$, thus $\Delta\sigma_{\text{ph}}/\sigma_{\text{ph}}$ is essentially temperature independent as seen from Eq. (5) and also shown in Figs. 4 and 7. The decrease of $\Delta\sigma_{\text{ph}}/\sigma_{\text{ph}}$ above 250 K is probably due to the higher rate of spontaneous spin flips in this range which reduces the influence of the microwave field. Since by reducing the spin density $\Delta\sigma_{\text{ph}}$ behaves in the same way as σ_{ph} itself, we conclude that the transition between trapped electrons and neutral dangling bonds is the only important recombination transition which determines the photoconductivity in high-defect-density material. For low-defect-density material, however, the diffusion rate of holes r_h to D^- states becomes comparable to r_e , and at low temperatures r_h will eventually govern the recombination process.

It should be noted that a quantitative description of the photoconductivity must include the random location of defects and trapped carriers in terms of the distributions in the tunnel and diffusion rates. In order to identify the dominant recombination processes, our qualitative treatment is sufficient. The importance of the hole diffusion process is further corroborated by thermal and infrared quenching effects found in low-defect-density material.^{15,22,23} Since activation of trapped holes into extended states by infrared or thermal excitation acts as a bypass of the slower diffusion process in localized states, this also supports our model for recombination in undoped a -Si:H that, depending on spin density and temperature, the tunneling and diffusion transitions are the essential recombination steps that determine the lifetime of the charge carriers rather than direct capture of free carriers by neutral dangling bonds.

ACKNOWLEDGMENT

We thank J. Beichler for preparing the samples.

*Permanent address: Physikalisch-Technische Bundesanstalt, Postfach 3345, D-3300 Braunschweig, Federal Republic of Germany.

¹H. Mell, B. Movaghar, and L. Schweitzer, *Phys. Status Solidi B* **88**, 531 (1978).

²R. A. Street, D. K. Biegelsen, J. C. Knights, C. Tsang, and R. M. White, *Solid State Electron.* **21**, 1461 (1978).

³I. Solomon, D. K. Biegelsen, and J. C. Knights, *Solid State Commun.* **22**, 505 (1977).

⁴E. A. Schiff, in *Tetraedrally Bonded Amorphous Semiconductors, Carefree, Arizona, 1981*, a Topical Conference on Tetrahedrally Bonded Amorphous Semiconductors, edited by R. A. Street, D. K. Biegelsen, and J. C. Knights (AIP, New York, 1981).

⁵K. Morigaki, D. J. Dunstan, B. C. Cavenett, P. Dawson, J. E. Nicholls, S. Nitta, and K. Shimakuwa, *Solid State Commun.* **26**, 981 (1978).

⁶D. K. Biegelsen, J. C. Knights, R. A. Street, C. Tsang, and R. M. White, *Philos. Mag. B* **37**, 477 (1978).

⁷K. Morigaki, Y. Sano, and J. Hirabayashi, *Solid State Commun.* **39**, 947 (1981).

⁸S. Depinna, B. C. Cavenett, T. M. Searle, and J. G. Austin, *J. Phys. (Paris) Colloq.* **C4**, 323 (1981).

⁹R. A. Street, *Phys. Rev. B* **26**, 3588 (1982).

¹⁰R. A. Street, *Philos. Mag. B* **46**, 273 (1982).

¹¹B. Movaghar, B. Ries, and L. Schweitzer, *Philos. Mag. B* **41**, 159 (1980).

¹²B. Movaghar, B. Ries, and L. Schweitzer, *Philos. Mag. B* **41**, 141 (1980).

¹³B. Movaghar and L. Schweitzer, *J. Phys. C* **11**, 125 (1978).

¹⁴L. Katz and A. S. Penfold, *Rev. Mod. Phys.* **24**, 28 (1952).

¹⁵H. M. Welsch (unpublished).

¹⁶W. Rehm, R. Fischer, J. Stuke, and H. Wagner, *Phys. Status Solidi B* **79**, 539 (1977).

¹⁷H. Dersch, J. Stuke, and J. Beichler, *Phys. Status Solidi B* **105**, 265 (1981).

¹⁸D. Weller, H. Mell, L. Schweitzer, and J. Stuke, *J. Phys. (Paris) Colloq.* **4**, 143 (1981).

¹⁹H. Dersch, J. Stuke, and J. Beichler, *Phys. Status Solidi B* **107**, 307 (1981).

²⁰L. Schweitzer, M. Grünwald, and H. Dersch, *Solid State Commun.* **39**, 355 (1981).

²¹W. B. Jackson, *Solid State Commun.* **44**, 477 (1982).

²²P. E. Vanier and R. W. Griffith, *J. Appl. Phys.* **53**, 3098 (1982).

²³P. E. Vanier, A. E. Delahoy, and R. W. Griffith, in *Tetraedrally Bonded Amorphous Semiconductors, Carefree, Arizona, 1981*, a topical conference on Tetrahedrally Bonded Amorphous Semiconductors, edited by R. A. Street, D. K. Biegelsen, and J. C. Knights (AIP, New York, 1981).